ADVANCED MATERIALS
www.advmat.de

Materials Views
www.MaterialsViews.com

Carbon Nanotubes: Measuring Dispersion and Length

Jeffrey A. Fagan, Barry J. Bauer, Erik K. Hobbie, Matthew L. Becker, Angela R. Hight Walker, Jeffrey R. Simpson, Jaehun Chun, Jan Obrzut, Vardhan Bajpai, Fred R. Phelan, Daneesh Simien, Ji Yeon Huh, and Kalman B. Migler*

Advanced technological uses of single-walled carbon nanotubes (SWCNTs) rely on the production of single length and chirality populations that are currently only available through liquid-phase post processing. The foundation of all of these processing steps is the attainment of individualized nanotube dispersions in solution. An understanding of the colloidal properties of the dispersed SWCNTs can then be used to design appropriate conditions for separations. In many instances nanotube size, particularly length, is especially active in determining the properties achievable in a given population, and, thus, there is a critical need for measurement technologies for both length distribution and effective separation techniques. In this Progress Report, the current state of the art for measuring dispersion and length populations, including separations, is documented, and examples are used to demonstrate the desirability of addressing these parameters.

1. Introduction

Single-walled carbon nanotubes (SWCNTs) are among the most promising nanomaterials, with projected uses in electronics, composites, sensor, and biomedical applications. Hindering the technological development and commerce of SWCNTS has been the fact that SWCNT properties vary significantly with the distribution of lengths, wrapping vectors, and dispersion state within a given sample, and the difficulty in measuring these parameters. Thus, to fully realize the benefits of using SWCNTs in an advanced technology, it is highly desirable to carefully control the type and number of nanotubes needed for a specific application. Reaching this goal requires both the methods to separate the desired materials from a given lot and the measurement science to direct intelligent efforts in producing them. Beginning in 2004, researchers at the National Institute of Standards and Technology (NIST) have focused on separating SWCNTs by factors such as dispersion, length, and diameter, and then refining the measurement science of SWCNTs through characterization of those improved populations.

Much of the difficulty in measuring carbon nanotubes comes from the wide number of possible nanotube types, with approximately several hundred single-walled tubes thought to be structurally stable at room temperature and pressure, as well as the innumerable varieties of double-walled and multiwalled nanotubes, each of which may be valuable for a specific use. To keep track of the different species of nanotubes the notation (*n*,*m*) is used, in which *n* and *m* describe the vector in hexagonal elements for rolling up a sheet of graphene to form the cylindrical nanotube. In accordance with the wide range of possibilities, many different methods for directing SWCNT synthesis have been pursued, resulting in a large number of manufacturers bringing a wide variety of difficult to compare nanotube soots onto the market. Unfortunately for characterization purposes, these SWCNT soots have often had notoriously low overall quality, with highly variable properties and significant impurity contents. Moreover, application of these soot materials to address issues such as environmental, health, and safety (EHS) concerns has led to significant uncertainty regarding their suitability for commercial use, and the kinds of controls necessary for harnessing SWCNTs in technological applications.

To combat the problem of polydispersity and the uncertainty in the measurement science, we decided to focus on using established techniques from the polymers, colloids, and material science fields to separate different SWCNT soots into fractionated populations through liquid-phase processing. Characterization of the fractionated populations is then used as feedback for the measurement science and separation technologies in a continuous cycle of improvement. The key to a liquid phase processing approach is the achievement of individualized dispersion of the nanotubes.

Dr. J. A. Fagan, Dr. B. J. Bauer, Dr. E. K. Hobbie, Dr. M. L. Becker[+], Dr. J. R. Simpson,[†] Dr. J. Chun,[‡] Dr. J. Obrzut, Dr. V. Bajpai,[¥] Dr. F. R. Phelan, Dr. D. Simien,[§] Dr. J. Y. Huh, K. B. Migler
Polymers Division
National Institute of Standards and Technology
Gaithersburg, MD 20899, USA
E-mail: Jeffrey.fagan@nist.gov
Dr. A. R. Hight Walker
Optical Technology Division
National Institute of Standards and Technology
Gaithersburg, MD 20899, USA
[+] Present Address: Department of Polymer Science
University of Akron, Akron, Ohio 44325, USA
[†] Present Address: Physics Department,
Towson University, Towson, MD 21252, USA
[‡] Present Address: Pacific Northwest National Lab
902 Battelle Blvd., P.O. Box 999, Richland, WA 99352, USA
[¥] Present Address: Seldon Technologies Inc.
Windsor, VT 05089, USA
[§] Present Address: Mechanical and Aerospace Engineering Department
West Virginia University, Morgantown, WV 26506, USA

DOI: 10.1002/adma.201001756

2. Dispersion[1]

Stable, individualized dispersion of nanotubes in a liquid phase can be accomplished through two methods. One of these methods, true formation of a solution, i.e., a negative free-energy change in mixing, $\Delta G_{mix} < 0$, has only recently been demonstrated,[2,3] and individualization occurs only for small concentrations of SWCNTs less than 20 μg mL^{-1}. The second method is to solubilize the SWCNT through the use of a dispersant material.[4] For dispersants that are small molecule surfactants, the partitioning of the soluble surfactant onto the SWCNT surface often occurs near the concentration of the critical micelle concentration for the surfactant. In the simplest sense, the physical mechanism behind the dispersal is that the surfactant forms a complete, or nearly complete, layer that stabilizes separated SWCNTs from reaggregation due to van der Waals forces; if the solution surfactant concentration is lowered, the surfactant leaves the surface and the SWCNTs will reaggregate. The density of the surfactant packing,[5,6] and the ease with which the surfactant can be removed from the surface, are then thought to determine the quality of the surfactant. Larger molecule dispersants, such as DNA or polymers, are hypothesized to act somewhat differently, as the absorption can be nearly irreversible. However, unless rearrangement of the molecule on the surface can occur there are likely to be gaps that can enable reaggregation. In either case for dispersant stabilization, the free energy of the initial individualization is still positive, and, thus, must be driven through external processing such as sonication (ultrasound).

Many reviews and experimental comparisons have been published for different small-molecule surfactants,[7–9] adsorbing macromolecules, and various polar and nonpolar solvents. Often the measurement of dispersion is performed using optical methods, such as ultraviolet-visible-near-infrared (UV-vis-NIR) absorbance spectroscopy, near-infrared (NIR) fluorescence, and Raman scattering. Of these methods UV-vis-NIR absorbance is the most commonly used. In our efforts we find that UV-vis-NIR measurements are particularly valuable as a quick screening tool;[10,11] an example of a set of spectra taken after sonication, then after purification by centrifugation, and the difference between the two for a small-diameter SWCNT sample (loaded at 1 mg mL^{-1}) in 2% (mass/volume) sodium deoxycholate (DOC) is shown in **Figure 1**. Unless stated otherwise, the standard uncertainty throughout this contribution is denoted by error bars equal to one standard deviation.

In general, a measured spectra after sonication yields information about the effectiveness of a surfactant for dispersing carbon (or in the highly effective limit, the fractional carbon concentration) and the diameter distribution of the sample. Performing a second measurement after a centrifugation step, which eliminates most larger SWCNT bundles, less effectively dispersed, and/or denser graphitic or amorphous carbon, as well as most catalytic impurities, allows for evaluation of the approximate dispersed mass fraction (from the fractional change in absorbance), the selectivity of the surfactant (through loss in optical transition intensity), and a combination of the individualization and length of the dispersed population (through size and sharpness of peaks).

Jeffrey A. Fagan is the project leader for single-walled carbon nanotubes research at the National Institute of Standards and Technology (NIST) in Gaithersburg, Maryland. He earned his BS degree in chemical engineering from the Johns Hopkins University in 2000, and his PhD in chemical engineering from Carnegie Mellon University in 2005. Afterwards, he was a National Research Council postdoctoral fellow at NIST from 2005 to 2007.

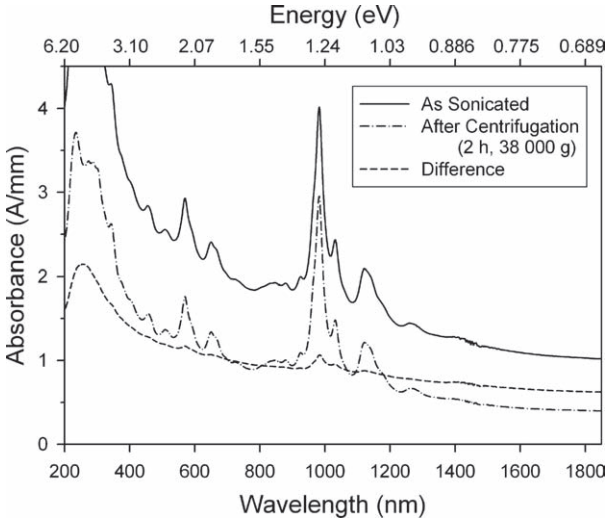

Figure 1. Absorbance spectra for a dispersed suspension of small diameter SWCNTs in 2% (mass/volume) sodium deoxycholate after sonication only (loaded at 1 mg mL^{-1} soot), after sonication plus centrifugation (2 h, at ≈372 400 m s^{-2}), and the difference between the two. The spectra of the two samples were measured on diluted aliquots (sonicated only: 1 part to 2 parts 2% DOC; centrifuged: 1 part to 1 part 2% DOC) before measurement to ensure linearity of the measurement. Scaled spectra, shown in the figure to represent full concentration, from the diluted fractions were found to overlay the absorbance of the undiluted aliquots in the region of concentration linearity (absorbance less than approximately 2.5 mm^{-1}). The approximate fraction of retained spectral weight after centrifugation between peak features measured at 775 nm is 0.48. Note that the majority of the peak feature spectral weight is retained upon centrifugation, indicative of strong selectivity by the surfactant for SWCNTs as opposed to carbonaceous impurities. Error bars are smaller than the linewidths.

In the example shown in Figure 1, the peaks are sharp and the optical transitions can easily be identified as: E^S_{11} (1320 to 800 nm), E^S_{22} (770 to 520 nm), and E^M_{11} (540 to 425 nm). Contributions below 425 nm contributions are overlapping E^S_{33}, E^M_{22}, E^S_{44}, and higher order transitions. The diameter distribution in this example is heavily weighted to diameters less than 1 nm, with the (6,5) SWCNT, E^S_{11} at 982 nm, being the dominant species. For larger diameter SWCNTs, the optical transitions

shift to lower energies (longer wavelengths), approximately inversely proportionional to the SWCNT diameter. Comparison of the spectra before and after centrifugation shows that ≈40% of the nonpeak absorbance is retained and ≈95% of the peak absorbance is retained. Although many manufacturers claim high-percentage carbon purity as SWCNT, an apparent percentage of 48% via this metric is above average for the batches we have tested. For a sample that was less well-dispersed, the total absorbance would be remarkably reduced, and the intensity of the peaks would be smaller. However, as full dispersion is approached, the resolution of transmittance as a metric for dispersion decreases. This is because different surfactant species provide different homogeneities of dielectric environments, which can broaden the spectral features even in the limit of full individualization.

Typically, as full individualization of the nanotubes is approached, a transition in measurement techniques is made to utilize NIR fluorescence. The intrinsic NIR fluorescence of the dispersed SWCNTs, first reported by Bachillo et al.,[4] has been shown to be remarkably sensitive to the dispersion state. It is hypothesized that the presence of a metallic SWCNT within a small bundle will completely quench the NIR emission of adjoining semiconducting SWCNTs, and that the fluorescence of small bundles containing only semiconducting SWCNTs will be significantly reduced by multiple-tube effects. An example of a 2D excitation versus emission plot for the sample shown in Figure 1 is presented in **Figure 2**.

NIR fluorescence is most useful in uniquely identifying the semiconducting SWCNTs present in a sample; the feature intensities can also provide approximate information about relative concentrations in the population, however, eliminating so-called "in-filter" effects, such as reabsorption of emitted photons, is difficult and the fluorescence cross sections are likely to be dispersant-sensitive.[12] An excellent example of this is shown in **Figure 3**. In Figure 3, the absorbance and fluorescence spectra are shown for two SWCNT samples prepared from a single nanotube batch, length-sorted to select for equivalent average lengths, and measured at equal concentrations, but dispersed using two different dispersants. Although both samples are believed to be completely individualized, based on

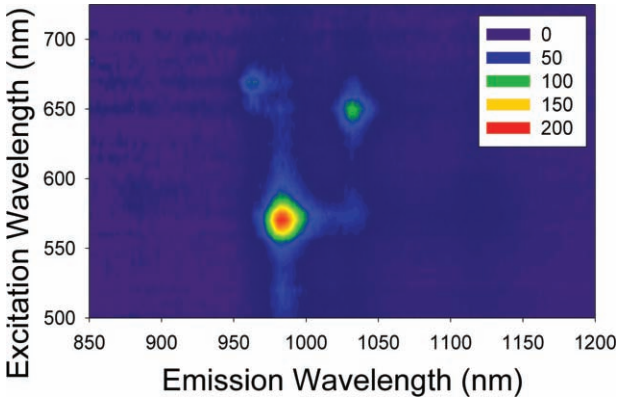

Figure 2. Emission versus excitation map for the centrifuged sampled shown in Figure 1, diluted to an absorbance of 0.03 per cm at 775 nm. At this dilution the sample appears almost completely transparent. Features due to the (6,5), and (7,5) are clearly visible.

neutron scattering measurements of similar solutions, the fluorescence intensity of the DOC dispersed sample is greater by a factor of 2.2, likely due to extrinsic effects such as the homogeneity of the surface environment.

Due to extrinsic effects, comparison of the fluorescence intensity of samples with different dispersants can be difficult to interpret. However, for samples of the same surfactant (and parent SWCNT soot) with different processing, fluorescence can be an effective metric for determining relative dispersion or chiral selectivity. We found this to be the case when comparing the dispersion in composites cast from solutions of different pH polymer solutions.[11] Absorbance and Raman spectroscopy were not able to identify changes in the dispersion, but fluorescence measurements showed a decrease in fluorescence intensity for samples cast from higher pH solutions; these composites were then found to have poorer dispersion via small angle neutron scattering.

Another benefit of fluorescence is that samples can be measured from single nanotubes,[13] whereas UV-vis-NIR absorbance typically requires concentrations above 10 μg mL^{-1} for robust measurement, and small angle neutron scattering effectively requires around 100 μg mL^{-1} for well-dispersed samples. The ability to measure such samples however should be used cautiously. It is well-established that many dispersant agents as well as various solvents will effectively disperse sufficiently dilute preparations. Measurement of apparently significant fluorescence at low nanotube concentrations does not necessarily indicate that the dispersant will effectively function at greater concentrations.[9] A minimum appropriate validation for the higher concentration solution, such as an identical absorbance-to-concentration ratio for the entire wavelength range at both concentrations, should additionally be measured in this instance.

Small angle scattering is a definitive measure of SWCNT dispersions. Small angle neutron[11,14,15] or X-ray[16] scattering (SANS or SAXS) can probe dispersions in liquids[15,14] or in solids,[11] and are very sensitive to contaminations of small amounts of clustered nanotubes. In brief, for a suspension of isolated rigid rods, the power law scaling for the scattered intensity versus scattering vector, q, is −1; loose networks of rods display a power law of −2, while denser aggregates display power laws up to −4. Measurement of a −1 slope over a significant q range, especially at small q, is thus significant evidence for bulk individualization of the SWCNTs. The scattering of larger structures increases at low q much more rapidly than the scattering from rigid rods. Therefore very small amounts of large contaminants will show up at low q.

Shown in **Figure 4** is the small angle scattering for 0.035 mg mL^{-1} SWCNTs in a polyacrylic acid (PAA) matrix prepared from aqueous solution at different pH values. While individual SWCNTs predominate in both samples, as is evident by the−1 power law in both cases, the sample prepared at pH 4.1 shows an increase in scattered intensity at low q which indicates that clusters are present. Both SANS and SAXS can measure such dispersions, but the weak scattering requires large samples and a scattering time of several hours.

Other techniques, including multiangle light scattering (MALS), dynamic light scattering (DLS), and separation techniques such as field-flow fractionation, can also be used to

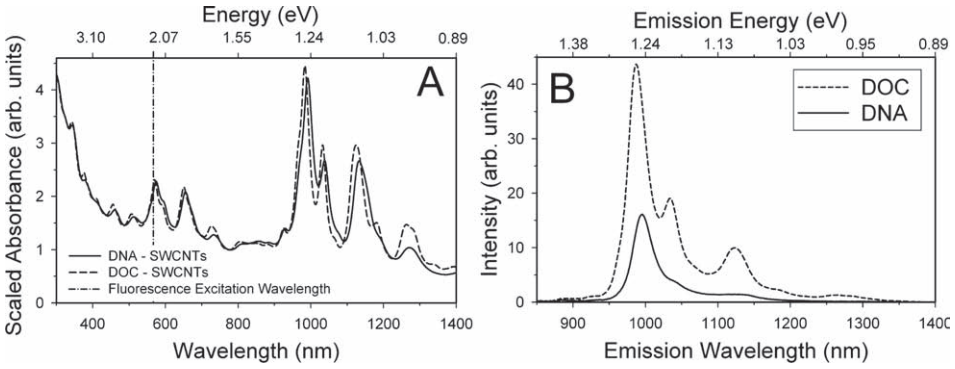

Figure 3. Comparison of absorbance and fluorescence spectra for two samples of SWCNTs dispersed in DNA and DOC. Although the absorbance spectra are similar and the fluorescence comparison was optimized for the fluorescence of the DNA-wrapped sample (568 nm excitation), the absolute intensity of the fluorescence from the DOC dispersed sample is significantly larger. Both samples are thought to be equally well dispersed, and were length-sorted to select for an average length of approximately 560 nm. The difference in the fluorescence is attributed to extrinsic effects such as a difference in surface coverage homogeneity. Error bars are smaller than the linewidths. Adapted with permission from [12]. Copyright 2009, Elsevier.

measure dispersion. Measurement of poorly dispersed or aggregating samples can be monitored, since aggregates are typically much larger than an individualized SWCNT in solution and thus scatter more light, or in the case of hydrodynamic-based separations, elute at times indicative of large particles. Specifically for dynamically aggregating samples, DLS is sometimes measured to compare changes in the aggregation state with time,[17] such as for environmentally driven aggregation.

For well-dispersed or chromatographically purified samples, MALS has the advantage over either SAXS or SANS of having a strong contrast between the SWCNTs and the liquid. Even for well-dispersed SWCNTs, this scattering is strong enough to make online measurements possible downstream of separation methods, such as size-exclusion chromatography (SEC)[18] and field-flow fractionation (FFF).[19] These separation techniques are efficient at removing large structures so that the scattering is characteristic of rods. One major difficulty with measuring these samples using light scattering is that the interaction of light with SWCNTs is very complex. Thus, interpretation of the light-scattering intensity and angular shape is difficult for unknown SWCNT mixtures.[17,18] Use of an FFF system to characterize SWCNT populations for quality control purposes is a subject of a forthcoming contribution from the NIST research group.

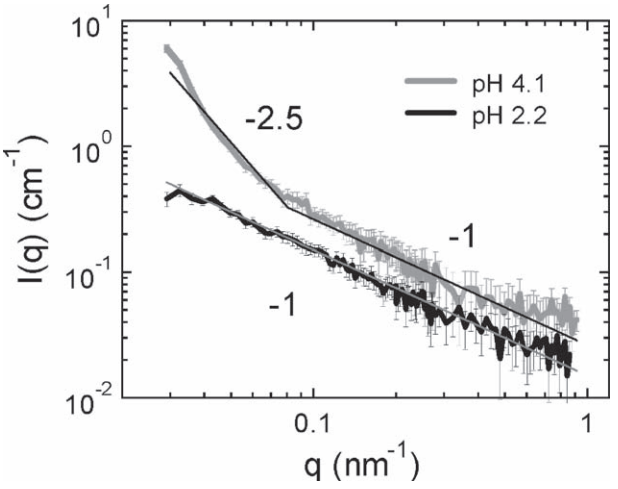

Figure 4. SANS intensity as a function of scattered wave vector for 0.035% SWNT (by mass) PAA composites cast from DNA-stabilized SWNTs in unbuffered (pH 2.2) and buffered (pH 4.1) aqueous 240 k PAA solution. Black lines denote a power law with an exponent of −1, and the gray line indicates a power law with the exponent −2.5. The black trace has been shifted slightly down by a constant multiplication factor of 1.77 for clarity. Error bars denote two standard deviations in the total experimental uncertainty. Reproduced with permission from [11]. Copyright 2006, ACS.

3. Diameter and Electronic Property Separation and Characterization

A recent review by Mark Hersam[20] outlines the significant efforts across the SWCNT community to separate mixed populations by their diameter, helicity, and electronic properties. In short, research has been conducted on the use of many different "handles" for separation, such as diameter,[21–24] helicity[25,26] and electronic property-based density differences, differences in affinity to column packing[27–29] or gel materials,[30,31] polarizability differences,[32,33] and differences in chemical reactivity.[34] Particularly good separation for milligram-sized quantities has been demonstrated using density-gradient ultracentrifugation, exploiting surfactant-sensitive density differences between different SWCNTs, and by ion-exchange chromatography (IEX), which exploits chirality-dependent interactions between DNA-wrapped SWNTs and the IEX resin.[27–29] Of these two methods we have typically focused on ultracentrifugation for preparing chirality or electronic-type separation.

As previously described,[20,21] density-gradient ultracentrifugation relies on differences in the effective buoyancies within a SWCNT population to provide a handle for separation. The effective densities in solution necessarily include the effects of the dispersant, and potentially the solvent, in determining the density of a given chirality tube; modification of the effective density dependence within a population through the use of multiple surfactants thus allows for separations, such as by electronic type. The significant series of results from Arnold et al.,[21] Green et al.,[35] and Yanagi et al.,[36] as well as our own

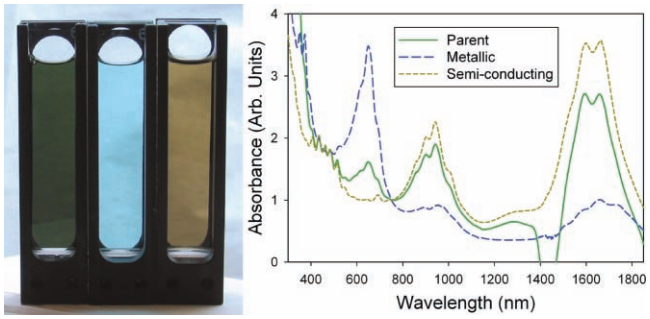

Figure 5. An example of density-gradient ultracentrifugation using cosurfactants for separation by electronic type. The green parent suspension was fractionated into the yellow, primarily semiconducting SWCNT fraction and a blue, primarily metallic SWCNT fraction. The daughter solutions were then dialyzed by forced filtration into 1% DOC. Spectra demonstrate the enrichment of the metallic species, with optical transitions in the 600 nm region, and the semiconducting species, with optical transitions in the 800 nm to 1100 nm and 1400 nm to 1800 nm regions. Spectra are linearly scaled such the $A(775\ \text{nm}) = 1$, for ease of comparison. The dip in the parent-solution absorbance at 1450 nm is an artifact from the background water spectrum subtraction, due to remaining density gradient media in the suspension. Reproduced with permission from [38]. Copyright 2009, ACS.

results shown in **Figure 5**, demonstrate that dramatic changes in separations can be driven by the number and type of dispersants used, the identity of the solvent and density gradient medium, the temperature, and the amount of equilibration time in the cosurfactant prior to separation. The hydrostatic pressure during centrifugation also appears to have an effect.[37] A quick survey of the literature for this method also makes it obvious that certain separations are easier, or at least better technically described, such as the separation of laser-ablation-synthesized metallic and semi-conducting SWCNTs, whereas the separation of <1 nm diameter SWCNTs by their electronic properties is more challenging. Conversely, separation by chirality appears to be easier for SWCNTs <1 nm in diameter.

Although in general NIST efforts have focused less on measurements that rely upon chirality and/or electronic type enrichment, changes in the chirality distribution are typically measured using UV-vis-NIR absorbance and fluorescence (using extended detectors), and using Raman spectroscopy. In UV-vis absorbance measurements the distribution of the peaks, which is related to the electronic transitions of the different SWCNT chiralities, changes during chirality-based separation. An example of this is shown in Figure 5 for laser ablation SWCNTs separated using cosurfactants and density-gradient ultracentrifugation.

UV-vis-NIR is particularly powerful for quickly assessing separations by electronic type or assessing separations with large changes in the diameter distribution. For smaller changes in the distribution, or for SWCNTs with overlapping optical absorbance features, resonant Raman spectroscopy and NIR fluorescence (semiconducting SWCNTs only) can provide higher resolution. Resonant Raman spectroscopy and NIR fluorescence are better than absorbance at specifying the SWCNTs in a population because each feature provides two pieces of information at a given excitation wavelength. In Raman scattering measurements, the frequency of the radial breathing mode (RBM) allows for specification of the diameter which, along with the resonance energy, is enough information to assign many SWCNTs. In fluorescence measurements, both the excitation energy and the emitted wavelength are known. Raman and fluorescence become especially useful in populations of tubes for which the diameter is larger than 1 nm, due to the increased number of possible chiral vectors with similar optical transitions. Unfortunately many Raman and fluorescence instruments are wavelength-limited and cannot effectively measure populations with diameters significantly larger than 1.2 nm. In these instances sequential separation of the population by electronic type and diameter, followed by absorbance spectroscopy may yield the best characterization of the diameter distribution. In any case, care should be taken for absolute assignments of *n*,*m* indices, particularly if there are a large number of potential matches to the excitation–emission profiles, if the effect of the dispersant on the energy of the transitions has not been accounted for, or if only a single excitation line is available.

4. Length Separation and Characterization

The primary component of research into SWCNTs conducted in the Polymers Division at NIST has been in the separation by and measurement of SWCNT length in a dispersed population.[14,18,39,40] As with chiral-angle separations, many different methodologies have been developed to produce length fractions. The most common technique has been SEC, along with separations based on field-flow fractionation, gel electrophoresis, and ultracentrifugation; intentional degradation is also used for producing shortened materials. Of these methods, ultracentrifugation, first described for length separation of SWCNTs at NIST, and intentional degradation have the largest demonstrated mass throughputs, while FFF and SEC offer the highest length resolution. Characterization of the SWCNT length in the produced fractions is typically performed through the use of atomic force microscopy (AFM), MALS, and depolarized DLS in the *Vh* configuration, along with occasional use of transmission electron microscopy (TEM). Other techniques, such as electrospray differential mobility analysis[41] (ES-DMA), have also been reported.

SEC in the literature and at NIST has primarily been conducted following the groundbreaking results of Zheng et al.[42,43] In the typical methodology a single-stranded DNA (ssDNA) dispersed population of SWCNTs is introduced to a column, or set of columns, containing porous packing material. The pore sizes are chosen to selectively allow only particles smaller than a given size to access the stagnant volume with the pores. Thus, as the initial plug injection travels through the column set with the bulk flow, the smaller SWCNTs preferentially sample the quiescent volume within the pores and thus have a delayed elution time. Over the length of several columns (in our setups approximately 75 cm) this effect is sufficient to generate narrow fractions of different length SWCNTs. An example of the separation achievable in a three column set is shown in **Figure 6**.

The benefits of size-exclusion chromatography are that it produces a highly reproducible length fraction with narrow distributions in a concentration range where online measurements such as MALS, UV-vis absorbance, and refractive index

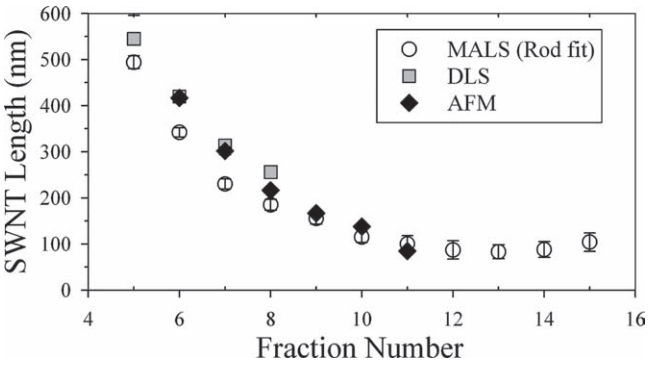

Figure 6. Average size versus elution time for a Sepax CNT three column set as measured by AFM, DLS, and MALS. Separation was described previously. Reproduced with permission from [18] and [39]. Copyright 2008, ACS, and Copyright 2007, ACS.

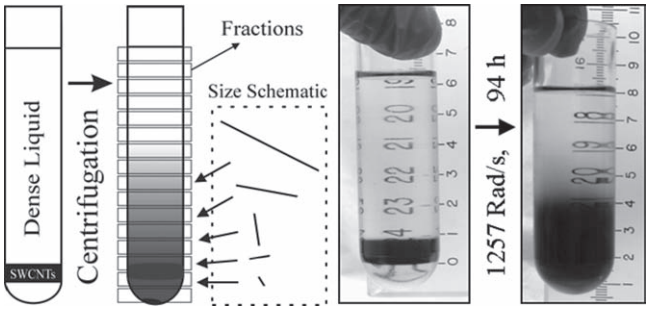

Figure 7. A schematic of length separation via centrifugation, and an example experiment. The example shown is for DOC dispersed SWCNTs spun at 1257 rad s^{-1} in a SW-32 rotor for 94 h at 15 °C. Reproduced with permission from [14]. Copyright 2008, ACS.

changes can be easily measured for quality control. Additionally, due to the consistency of the method, it is easy to collect the narrow fractions for concentration and further processing. Unfortunately there are also significant limitations to the demonstrated SEC length fractionation for SWCNTs. These include: the necessity to use ssDNA as the dispersant, which can cost 50 to 100 times as much as the SWCNTs separated; the danger of losing expensive columns if the dispersion fails; a throughput <0.5 mg of total SWCNT capacity per 90 min run for a few thousand dollar column; the necessity to filter out many of the desirable long SWCNTs to avoid clogging the column; and the presence of some absorption–desorption behavior that tends to broaden the shorter SWCNT fractions. A major difficulty with SEC separations is that SWCNTs can be significantly larger than the polymers that are commonly separated by SEC. Large SWCNTs are poorly resolved by columns normally used for polymers which have an exclusion limit of approximately 600 to 700 nm.

Preparation of length fractions by ultracentrifugation,[14,40] primarily a focus of NIST research, although also used by Sun et al.,[44] is based on the fundamental difference in length scaling of the buoyancy and frictional forces for a rigid rod under creeping-flow conditions. At low Reynolds number, the frictional drag increases approximately proportional to $L/\ln(L/r)$, where L is the length of the nanotube and r is the radius, whereas the buoyancy always increases with the total effective volume (proportional to L for a rod). When a thin layer of dispersed SWCNTs is set in a liquid of significantly different density, such that the density difference to the liquid is essentially the same for all SWCNT chiralities, the response to applied centrifugation will be a migration of the dispersed SWCNTs with the longer SWCNTs moving faster; separation by length is then achieved by fractionating the liquid column after an appropriate length of time. A schematic of this process and an example experiment are shown in **Figure 7**.

Advantages of separation by ultracentrifugation are: it can separate SWCNTs up to at least several micrometers in length, larger mass throughput than SEC (roughly 10 mg per 24 h for our typical rotor), an ability to use relatively cheap dispersants such as DOC (≈$1 per g), reasonable length resolution (the typical standard deviation is ≈0.1 to 0.2 times $<L>$), low failure cost, compatibility with ultracentrifugation based chirality separations, and a manipulability for optimal separation of different length ranges. Downsides to ultracentrifugation are: the necessity to tune the separation for different diameter populations of SWCNTs or other nanotubes, such as double-walled nanotubes (DWCNTs); lower length resolution than SEC (typically limited by the vertical height of the injection layer); an inability for online detection and measurement during production; and the presence of instabilities, apparently due to reorganization of the surfactant under centrifugation that limit the usable separation rate to well-below achievable applied centripetal accelerations.

Characterization of the optical properties of dispersed SWCNTs separated through both SEC and ultracentrifugation has yielded a surprising length dependence in the apparent optical transition strength with SWCNT length. UV-vis-NIR absorbance measurements have shown that the strength of the SWCNT specific optical transitions linearly increase in relation to the apparent π-plasmon absorbance with SWCNT length. For SWCNTs longer than ≈600 nm, depending on the number and distribution of chiralities in the population, this effect causes the SWCNT solutions to become colored without chirality separation. An example of the colors obtained from various populations of ≈1 μm long SWCNTs, as well as a set of example spectra, are shown in **Figure 8**.

Because the fluorescence of the SWCNTs is coupled to the absorbance, the fluorescence of a dilute solution of SWCNTs also shows a linear increase with length. In terms of absolute quantum yield (QY), the relative increase in the optical transition strength compared to the background indicates that more excitons are formed per absorbed photon in the longer SWCNTs; thus, the QY, assuming a length-independent efficiency for emission of excitons via fluorescence, should increase. This helps to explain the abundance of more recent literature results on purified, and typically longer length, SWCNTs in solution that demonstrate a QY approaching 10%.[45,46] Although beyond the scope of this Progress Report, a possible explanation for an increase in oscillator strength with SWCNT length would be exciton delocalization, possibly related to the length of the nanotube with respect to the wavelength of the incident radiation. Current estimates of the size of a single exciton in semiconducting SWCNTs are around 1 nm, comparable to or slightly larger than the diameter of the most common single-walled nanotubes. Both the length of the SWCNT and the

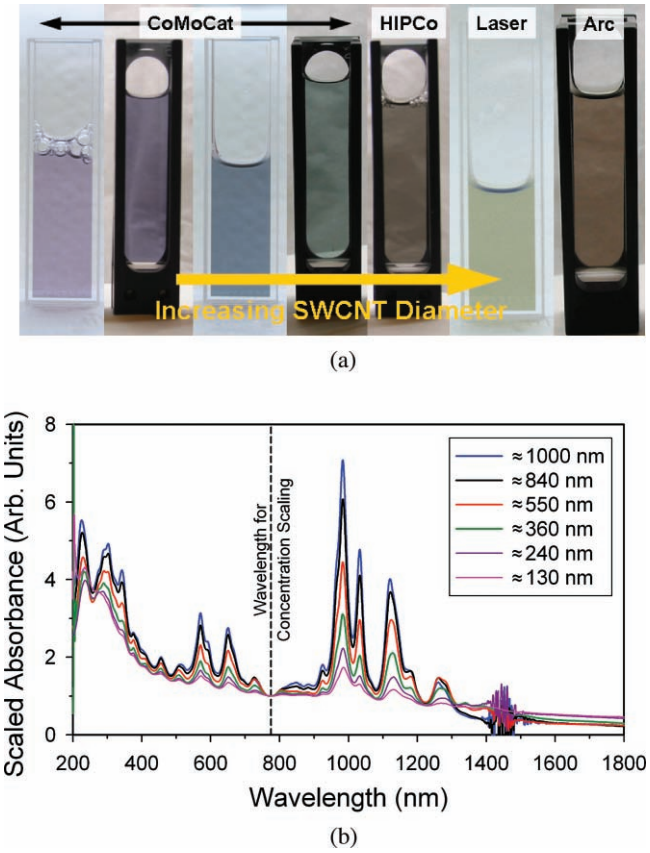

Figure 8. a) Photograph of colored-SWCNT dispersions comprised of ≈1 μm long SWCNTs in order of increasing average nanotube diameter. Note that these solutions have not been separated by chiral vector. The spectrum of the blue fraction, third from the left, is the spectrum of the longest fraction shown in (b). Left to right the parent soots for these dispersions are four different cobalt-molybdenum catalyst (CoMoCat) batches (SouthWest Nanotechnologies SG65-000-0002, SG65-000-0024, S-P95-2 NI-6-A001, SG76-31 k), a high pressure carbon monoxide (HIPCo) process batch (Carbon Nanotechnologies P286), laser ablation method SWCNTs (NASA batch 338), and electric-arc-produced SWCNTs (Carbolux). b) Absorbance spectra for length separated CoMoCat SWCNTs (batch S-P95-2 NI-6-A001), scaled by apparent π-plasmon absorbance at 775 nm. Reproduced with permission from [14]. Copyright 2008, ACS.

wavelength of the absorbed radiation are two-to-three orders of magnitude larger than this, pointing to multiple sites along a single SWCNT being capable of supporting a fundamental excitation. Another factor for short SWCNTs is the presence of end cap "defects," which can be the primary source of D-band Raman scattering,[12] and thus by inference, the primary defect sites, and which may serve to limit the formation of excitons in shorter SWCNTs. Interestingly, the apparent length-dependent optical effect appears to have an asymptote at a constant transition-to-background absorbance ratio for SWCNTs longer than approximately 1 to 1.2 μm. For SWCNTs longer than this threshold, the bulk result is consistent with fluorescence measured from directly imaged individual SWCNTs.[47] Fluorescence has also been used to measure the length of individualized SWCNTs in solution,[48,49] but has not been an area of active research at NIST.

For measurement of the size distribution of dispersed SWCNT populations, the most popular method is AFM, however the perhaps best method to date for relative size measurement is calibrated FFF. In AFM measurements, a small sample of the dispersion is deposited on a substrate, typically a silicon wafer or mica sheet, the surfactant is removed, and the sample is imaged in tapping mode. After imaging, the lengths of any nonoverlapping SWCNTs can be measured, although direct traceability for a measured value is uncommon. The primary difficulty and uncertainty in AFM measurement comes from the difficulty in depositing the SWCNTs, and in removing the surfactant without aggregating or altering the distribution of deposited SWCNTs. Unfortunately these difficulties tend not to be trivial. This is especially true for many surfactant-dispersed samples because the mass of surfactant in the sample can be orders of magnitude greater than the SWCNT concentration. There is also the potential difference in the probability of identifying SWCNTs of different lengths that may selectively bias measured values to longer lengths. Lastly, AFM is a time-intensive technique that is not suitable for routine screening of many samples, and, especially for quality control (QC) and process development purposes, a more facile and rapid method would be preferable.

FFF has the potential to provide the facile and rapid screening of size distributions necessary for process development and QC. FFF is a powerful method for characterizing the dispersion and length distribution of a SWCNT sample[19] because of the wide size range that is separable,[50] the small sample volume that is required, the ability to perform online characterization, and the quick results. A properly calibrated instrument, calibrated with reference particles of known size and appropriate hydrodynamic models, can provide relative size information for a dispersed-SWCNT sample in less than 90 min, with little preparation required between runs. In FFF, a focused volume of injected particles is forced to flow between two narrowly spaced plates. The most common implementation, flow-FFF, uses a porous bottom plate which allows the solvent to pass through, but is impermeable to suspended SWCNTs. A parabolic velocity profile is established between the plates, and the average position of the particles in the parabolic flow field governs the elution time. Separation occurs because of the increase in diffusivity with smaller hydrodynamic size; due to their larger diffusion coefficients, smaller particles tend to have greater excursions from the membrane surface, and are thus entrained at a higher rate in the parabolic flow acting in the elution direction. Particles with smaller effective hydrodynamic radii thus elute first, and larger particles elute later.[50–52] The ability to use any arbitrary function for the cross-flow strength with time allows for fine control of the elution rate and resolution of the size versus time dependence.

A common effect of many SWCNT processing techniques, such as acid refluxing and sonication, is a reduction in the length of the processed SWCNTs. When harnessed to purposefully produce shorter average length distributions, this is referred to as intentional degradation. In either instance, intentional or required shortening has important implications for the end properties of the processed material. Tracking the changes in the size distribution as a function of processing time, processing procedures, or synthesis conditions is thus

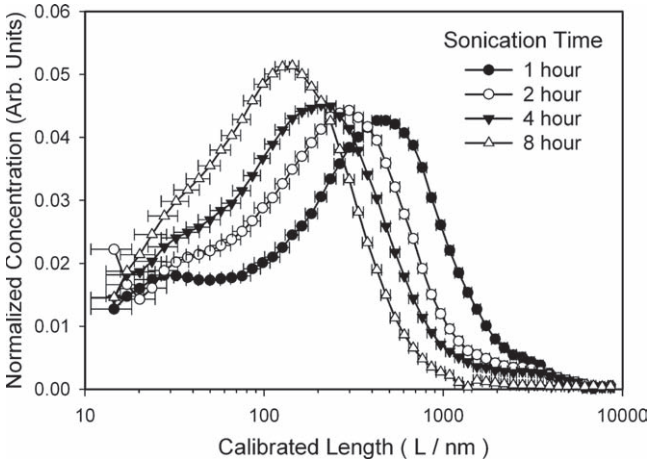

Figure 9. FFF characterization of intentionally shortened SWCNT dispersions produced through extended sonication. Extended sonication leads to a reduction in SWCNT length that can be rapidly characterized using FFF.

an important and desirable measurement. FFF appears to be nearly ideal for measuring such process-driven changes. As an example of the power of FFF, we conducted an experiment by sequentially increasing the sonication time, a common variable in SWCNT processing. The instrument is calibrated by using a suspension of latex spheres of known size and converting elution time to hydrodynamic size and then to rod length through an appropriate hydrodynamic theory. **Figure 9** is a plot of the length distribution for the same batch of SWCNTs exposed to an increasing sonication time. Extending the sonication time continually shortens the SWCNTs in this example. FFF is a convenient method for interrogating this type of processing effect.

Light-scattering techniques are another set of methods that we have used for characterizing the average lengths of different SWCNT dispersions. Two light-scattering methods are of significant interest, MALS and depolarized DLS. Of the two, DLS is more commonly reported in the literature, but is frequently abused as a measurement technique through disregard for the effects of the nanotube anisotropy on the validity of a single-angle unpolarized measurements. For well-dispersed dilute populations, multiangle cross-polarized (*Vh*) DLS provides a precise measurement of length, particularly for relatively narrow length distribution populations. The angular dependence of the *Vh* rotational correlation time is measured and used to calculate the mass-average SWCNT length. The thermal rotational relaxation time is obtained by fitting the measured autocorrelation function to an exponential decay, as shown in **Figure 10a**. This yields a wavevector (scattering angle) dependent relaxation rate (Figure 10b), with the zero-angle intercept, providing a measure of the thermal rotational diffusivity, D_r. The mean length is obtained from D_r by applying the Doi–Edwards theory for dilute suspensions of rigid rods. For aggregating solutions however, in which the time-dependent relaxation rate is measured to infer a relative size increase, it is obvious that multi-angle *Vh* measurements are unsuitable. Under those conditions it should be noted that it is unlikely that individual SWCNT size is being measured, and such data should be analyzed with that in mind.

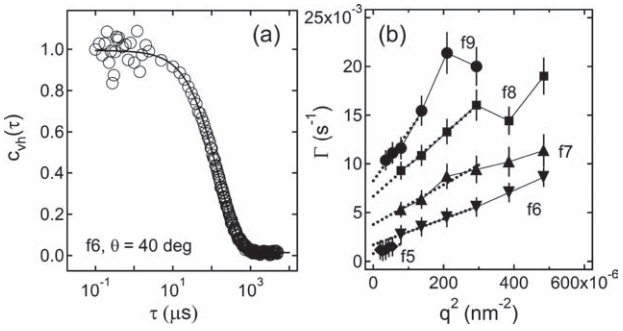

Figure 10. a) A typical *Vh* autocorrelation function for a DNA–SWCNT suspension that has been length-sorted by SEC. The exponential relaxation used to obtain the rotational diffusion rate is shown as a model fit to the data (solid line). b) Relaxation rate as a function of wavevector squared for five different SEC fractions (f5–f9) ranging in length from 100 to 600 nm and prepared through dispersion with ssDNA as described. Reproduced with permission from [39]. Copyright 2007, ACS.

Static light scattering in the form of online multiangle light scattering (MALS) can also be used to characterize the length distribution. Online measurements are made of SWCNT concentration, molar mass, and size (length) using UV-vis absorption combined with MALS as the nanotubes flow through the SEC column.[18] MALS data are fit with a polydisperse anisotropic rod scattering function that gives low polydispersity for most of the fractions. Higher polydispersities were obtained near the large size-exclusion limit and beyond the small size-exclusion limit of the SEC column. These fits indicate that the molar mass is linearly proportional to the rod length over a wide range of fractions, consistent with the expected rigid-rod behavior.

4.1. Examples of the Effects of SWCNT Length

Measurement technology for the determination of length distribution is particularly critical due to the effects of SWCNT length for many important phenomena, such as cellular interactions, percolation thresholds, strength of interactions with external fields, self assembly, and optical strength. Of these the effects of SWCNT size on cellular interactions and uptake may be the most important, since EHS concerns may act as a limiting gateway to SWCNT technology development.

Extensive efforts in determining SWCNT toxicological properties, well outside the scope of this report, have been and continue to be reported in the literature. In our opinion, an underreported and important factor in determining these properties is the length distribution of the SWCNTs. Utilizing the well-dispersed and length-separated DNA-wrapped SWCNTs produced using SEC, we recently explored the effects of average length on cellular uptake and metabolism by several mammalian cell lines including a diploid primary human fibroblast cell line, IMR90, as well as A549 (human alveolar basal epithelial cells), MC3T3 (clonal murine calvarial), and A10 (embryonic rat thoracic aorta medial layer myoblasts) cells in an in vitro assay.[53] Utilizing a Wst-1 assay, our results indicated that only SWCNTs shorter than ≈200 nm negatively affected the metabolism, even at concentrated SWCNT loadings above 30 μg mL^{-1}, as indicated by

the converted amount of a formazan salt. Exploring this result further, we exchanged the DNA on a long and a short SWCNT population with DNA containing one of two fluorophore labels, and then measured the fluorescence inside exposed cells after incubation for 16 h and removal and exchange of the supernatant. Regardless of the tag chosen, we measured the presence of the tagged SWCNT only for exposure by the <200 nm average length population. The implication is that shorter SWCNTs are taken up by the exposed cell lines at a much greater rate and could have significantly different exposure effects than longer SWCNTs; by corollary, SWCNTs targeted for cellular uptake should be limited to those that transport relatively quickly to increase the dose effectiveness in areas such as medical therapeutic applications.

Another example of the influence of length distribution on SWCNT properties occurs in the manipulation of dispersed SWCNTs through alternating electric fields;[54] these fields can induce alignment of the nanotubes due to anisotropy in the polarizability as well as center of body motion through dielectrophoresis. In either effect, the frequency-dependent phase lag of the polarizability relative to the external field determines the direction of the rotational or body force induced on the SWCNT, but the length has extreme effects on the magnitude of the force. Our work was the first result to control for the length of the SWCNTs when measuring the anisotropic polarizability,[54] and we determined length control to be critical in extracting a meaningful value. By controlling for the length, the average degree of alignment for all of the SWCNTs in solution was made to be equivalent because longer SWCNTs align more than shorter SWCNTs, and thus we were able to use linear dichroism to measure the degree of alignment. Without control of the length, the distribution of alignments significantly modifies the apparent dichroism in a manner that is difficult to account for.

Measurement of the anisotropic polarizability is important because dielectrophoresis is a potentially scalable method for separating metallic and semiconducting SWCNTs. Although separations of metallic and semiconducting SWCNTs with high-frequency fields have been demonstrated, rational design for separations is severely limited without measured parameters for the frequency-dependent magnitude and direction of the polarizability. Currently we are working to measure the chirality-specific anisotropic polarizability as a function of length and frequency to map out the useful phase space for manipulation with AC electric fields.

A last example of the importance of length distribution metrology is in the control of network percolation in a thin film or bulk composite. Although it has long been understood for multiwalled nanotubes that the percolation threshold in 3D is reduced with longer nanotubes, no validation of the effects of length on the 2D percolation of high aspect ratio rods had been conducted. This is critical becuase properties, such as the optical transparency of such materials, depend upon the mass loading, and if percolation with similar conductivity can be demonstrated at lower SWCNT loadings it will increase the technological potential for applications.

Comparing length-sorted and mixed populations of dispersed SWCNTs, we found that the change in surface conductance closely followed the network percolation model, with the longest population demonstrating a significantly lower percolation threshold than the shorter fraction.[55] The universal percolation exponents obtained for the longer tubes conform well to the predictions of generalized effective medium (GEM) percolation theory in 2D. The critical conductivity percolation concentration of 0.018 μg cm^{-2} in these 2D networks is the lowest reported to date (**Figure 11**).

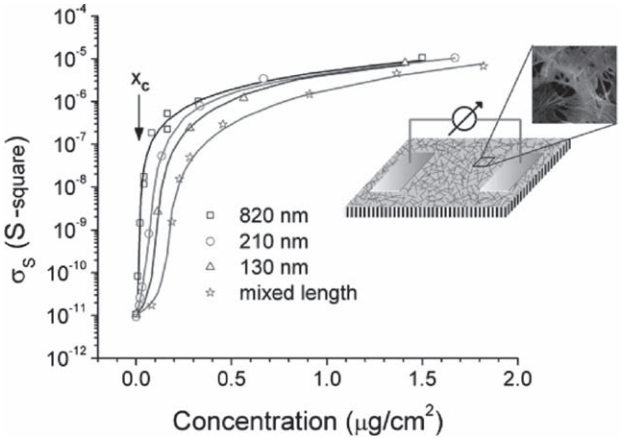

Figure 11. Conductivity as a function of surface concentration for length-sorted SWCNTs. The lines represent the conductivities fitted to the GEM-percolation model. Reproduced with permission from [55]. Copyright 2008, ACS.

Interestingly, the shortest fraction used in the experiment, $\langle L \rangle \approx 130$ nm, significantly outperformed the films produced from unsorted populations, despite the longer length, $\langle L \rangle \approx 230$ nm, of the mixed population. One explanation for this is that the mixed population percolates in a thin, but characteristically 3D, network. The universal percolation exponents calculated for the short- and mixed-length tube networks are both consistent with a 3D network. We hypothesize that separation reduces the potential build up of a network without percolation, and thus accounts for the improved performance. Overall, however, these results indicate that an increasing fraction of SWCNT connections are made in the third dimension in short tube networks.

In summary, network formation using sorted SWCNTs indicates that considerable control over the conductivity and optical properties can be obtained by adjusting SWCNT electronic type,[56] chiral vector,[35] length,[50] concentration, and polydispersity. GEM-percolation theory also provides a convenient framework for describing and engineering these changes for nanotechnology applications exploiting these novel materials.

5. Reference Materials

Knowledge gained in the development of separation technology and improved metrology has enabled the production of SWCNT reference materials to serve the metrology needs of academic, industrial, and regulatory concerns. NIST is expecting to release several grades of SWCNT reference materials in 2010, including a certified for elemental composition raw soot (SRM 2483), a purified "buckypaper" SWCNT reference material (RM 8282), and a set of length-separated populations in aqueous

dispersions (RM 8281). The characterization of these materials is informed by the knowledge gained through the characterization of factors such as the dispersion and length distribution detailed above, and should be a valuable resource to each of the different SWCNT user communities.

6. Summary and Outlook

The dispersion state and the length distribution of a SWCNT population are key parameters that determine the achievable properties from a given sample. Measurement technologies for and separation methodologies by these attributes are thus necessary to improve the commercial development of SWCNT technologies. The particular development of these technologies and methodologies at NIST has been the focus of this contribution, however several other organizations, including international bodies, such as the International Standards Organization (ISO) and the Versailles Project on Advanced Materials and Standards (VAMAS), as well as many academic and governmental research groups, are constantly improving the scientific understanding of SWCNT properties and processing. It is our view that the technological development of nanotubes has reached a point where the truly desirable fundamental properties of the nanotubes can be accessed through processing and characterization for high-value commercial applications. The release of well-characterized reference materials, standard protocols, and documentary standards is an additional enabling milestone that is rapidly approaching. Furthermore, ongoing research to facilitate more efficient and more selective isolation of desired SWCNT lengths and chiral vectors is likely to only accelerate the development of SWCNT materials into applications. In brief, the future of SWCNT materials appears to be bright and improving.

Acknowledgements

We acknowledge the support of the National Institute of Standards and Technology in providing the neutron research facilities referred to in this work, as well as initiative funding of the nanotube research. Additionally, many entities, including Southwest Nanotechnologies, Rice University, NanoPower Research, and NASA, among many others, have donated time and/or materials that have been gratefully received and contributed substantially to the course of this work. J.A.F. also gratefully acknowledges the support of a NIST National Research Council postdoctoral fellowship from 2005 to 2007. Official contribution of the National Institute of Standards and Technology; not subject to copyright in the United States. This article is part of a Special Issue on Materials Science at the National Institute of Standards and Technology (NIST).

Received: May 12, 2010
Published online: August 26, 2010

[1] Certain equipment, instruments, or materials are identified in this paper in order to adequately specify the experimental details. Such identification does not imply recommendation by the National Institute of Standards and Technology nor does it imply the materials are necessarily the best available for the purpose.

[2] S. D. Bergin, V. Nicolosi, P. V. Streich, S. Giordani, Z. Sun, A. H. Windle, P. Ryan, N. P. P. Niraj, Z. T. Wang, L. Carpenter, W. J. Blau, J. J. Boland, J. P. Hamilton, J. N. Coleman, *Adv. Mater.* **2008**, *20*, 1876.
[3] S. Giordani, S. D. Bergin, V. Nicolosi, S. Lebedkin, M. M. Kappes, W. J. Blau, J. N. Coleman, *J. Phys. Chem. B* **2006**, *110*, 15708.
[4] S. M. Bachilo, M. S. Strano, C. Kittrell, R. H. Hauge, R. E. Smalley, R. B. Weisman, *Science* **2002**, *298*, 2361.
[5] D. A. Tsyboulski, E. L. Bakota, L. S. Witus, J. D. R. Rocha, J. D. Hartgerink, R. B. Weisman, *J. Am. Chem. Soc.* **2008**, *130*, 17134.
[6] H. Cathcart, V. Nicolosi, J. M. Hughes, W. J. Blau, J. M. Kelly, S. J. Quinn, J. N. Coleman, *J. Am. Chem. Soc.* **2008**, *130*, 12734.
[7] M. F. Islam, E. Rojas, D. M. Bergey, A. T. Johnson, A. G. Yodh, *Nano Lett.* **2003**, *3*, 269.
[8] W. Wenseleers, I. I. Vlasov, E. Goovaerts, E. Obraztsova, A. S. Lobach, A. Bouwen, *Adv. Funct. Mater.* **2004**, *14*, 1105.
[9] R. Haggenmueller, S. S. Rahatekar, J. A. Fagan, J. Chun, M. L. Becker, R. R. Naik, T.Krauss, L. Carlson J. F. Kadla, P. C. Trulove, D. F. Fox, H. C. DeLong, Z. Fang, S. O. Kelley, J. W. Gilman, *Langmuir* **2008**, *24*, 5070.
[10] T. Kashiwagi, J. A. Fagan, J. F. Douglas, K. Yamamoto, A. N. Heckert, S. D. Leigh, J. Obrzut, F. Du, S. Lin-Gibson, M. Mu, K. I. Winey, R. Haggenmueller, *Polymer* **2007**, *48*, 4855.
[11] J. A. Fagan, B. J. Landi, I. Mandelbaum, J. R. Simpson, V. Bajpai, B. J. Bauer, K. Migler, A. R. H. Walker, R.Raffaelle, E. K. Hobbie, *J. Phys. Chem. B* **2006**, *110*, 23801.
[12] J. R. Simpson, J. A. Fagan, M. L. Becker, E. K. Hobbie, A. R. H. Walker, *Carbon* **2009**, *47*, 3238.
[13] D. A. Tsyboulski, S. M. Bachilo, R. B. Weisman, *Nano Lett.* **2005**, *5*, 975.
[14] J. A. Fagan, M. L. Becker, J. Chun, P. Nie, B. J. Bauer, J. R. Simpson, A. R. Hight Walker, E. K. Hobbie, *Langmuir* **2008**, *24*, 13880.
[15] B. J. Bauer, M. L. Becker, V. Bajpai, J. A. Fagan, E. K. Hobbie, K. Migler, C. M. Guttman, W. R. Blair, *J. Phys. Chem. C* **2007**, *111*, 17914.
[16] J. A. Fagan, J. R. Simpson, B. J. Landi, L. J. Richter, I. Mandelbaum, V. Bajpai, D. L. Ho, R. Raffaelle, A. R. Hight Walker, B. J. Bauer, E. K. Hobbie, *Phys. Rev. Lett.* **2007**, *98*, 147402.
[17] B. A. Smith, K. Wepasnick, K. E. Schrote, A. R. Bertele, W. P. Ball, C. O'Melia, D. H. Fairbrother, *Environ. Sci. Technol.* **2009**, *43*, 819.
[18] B. J. Bauer, J. A. Fagan, E. K. Hobbie, J. Chun, V. Bajpai, *J. Phys. Chem. C* **2008**, *112*, 1842.
[19] J. Chun, J. A. Fagan, E. K. Hobbie, B. J. Bauer, *Anal. Chem.* **2008**, *80*, 2514.
[20] M. C. Hersam, *Nat. Nanotechnol.* **2008**, *3*, 387.
[21] M. S. Arnold, S. I. Stupp, M. C. Hersam, *Nano Lett.* **2005**, *5*, 713.
[22] M. S. Arnold, A. A. Green, J. F. Hulvat, S. I. Stupp, M. C. Hersam, *Nat. Nanotechnol.* **2006**, *1*, 60.
[23] F. Hennrich, S. Lebedkin, M. M. Kappes, *Phys. Status Solidi B* **2008**, *245*, 1951.
[24] N. Stürzl, F. Hennrich, S. Lebedkin, M. M. Kappes, *J. Phys. Chem. C* **2009**, *113*, 14628.
[25] X. Peng, N. Komatsu, S. Bhattacharya, T. Shimawaki, S. Aonuma, T. Kimura, A. Osuka, *Nat. Nanotechnol.* **2007**, *2*, 361.
[26] A. A. Green, M. C. Duch, M. C. Hersam, *Nano Res.* **2009**, *2*, 69.
[27] M. Zheng, A. Jagota, M. S. Strano, A. P. Santos, P. Barone, S. G. Chou, B. A. Diner, M. S. Dresselhaus, R. S. McLean, G. B. Onoa, G. G. Samsonidze, E. D. Semke, M. Usrey, D. J. Walls, *Science* **2003**, *302*, 1545.
[28] M. Zheng, E. D. Semke, *J. Am. Chem. Soc.* **2007**, *129*, 6084.
[29] X. Tu, M. Zheng, *Nano Res.* **2008**, *1*, 185.
[30] D. A. Heller, R. M. Mayrhofer, S. Baik, Y. V. Grinkova, M. L. Usrey, M. S. Strano, *J. Am. Chem. Soc.* **2004**, *126*, 14567.
[31] T. Tanaka, H. Jin, Y. Miyata, S. Fujii, H. Suga, Y. Naitoh, T. Minari, T. Miyadera, K. Tsukagoshi, H. Kataura, *Nano Lett.* **2009**, *9*, 1497.
[32] R. Krupke, F. Hennrich, M. M. Kappes, H. v. Lóhneysen, *Nano Lett.* **2004**, *4*, 1395.

[33] D. H. Shin, J. Kim, H. C. Shim, J. Song, J. Yoon, J. Kim, S. Jeong, J. Kang, S. Baik, C Han, *Nano Lett.* **2008**, *8*, 4380.
[34] S. Ghosh, C. N. R. Rao, *Nano Res.* **2009**, *2*, 183.
[35] A. A. Green, M, C. Hersam, *Nano Lett.* **2008**, *8*, 1417.
[36] K. Yanagi, Y. Miyata, H. Kataura, *Appl. Phys. Express* **2008**, *1*, 034003.
[37] N. Nair, W. Kim, R. D. Braatz, M. S. Strano, *Langmuir* **2008**, *24*, 1790.
[38] E. K. Hobbie, J. A. Fagan, J. Obrzut, S. D. Hudson, *ACS Appl. Mat. Interfaces* **2009**, *1*, 1561.
[39] J. A. Fagan, J. R. Simpson, B. J. Bauer, S. Lacerda, M. L. Becker, J. Chun, K. B. Migler, A. R. Hight Walker, E. K. Hobbie, *J. Am. Chem. Soc.* **2007**, *129*, 10607.
[40] J. A. Fagan, M. L. Becker, J. Chun, E. K. Hobbie, *Adv. Mater.* **2008**, *20*, 1609.
[41] L. F. Pease, D. Tsai, J. A. Fagan, B. J. Bauer, R. A. Zangmeister, M. J. Tarlov, M. R. Zachariah, *Small* **2009**, *5*, 2894.
[42] M. Zheng, A. Jagota, E. D. Semke, B. A. Diner, R. S. McLean, S. R.Lustig, R. E. Richardson, N. G. Tassi, *Nat. Mater.* **2003**, *2*, 338.
[43] X. Y. Huang, R. S. McLean, M. Zheng, *Anal. Chem.* **2005**, *77*, 6225.
[44] X. Sun, S. Zaric, D. Daranciang, K. Welsher, Y. Lu, X. Li, H. Dai, *J. Am. Chem. Soc.* **2008**, *130*, 6551.
[45] J. Lefebvre, D. G. Austing, J. Bond, P. Finnie, *Nano Lett.* **2006**, *6*, 1603.
[46] S. Ju, W. P. Kopcha, F. Papadimitrakopoulos, *Science* **2009**, *323*, 1319.
[47] R. B. Weisman, "Quantitative Analysis of Bulk SWNT Samples using NIR-Fluorimetry", *Materials Research Society Presentation*, Boston, MA, November **2008**.
[48] D. A. Tsyboulski, S. M. Bachilo, A. B. Kolomeisky, R. B. Weisman, *ACS Nano* **2008**, *2*, 1770.
[49] J. P. Casey, S. M. Bachilo, C. H. Moran, R. B. Weisman, *ACS Nano* **2008**, *2*, 1738.
[50] F. R. Phelan, B. J. Bauer, *Chem. Eng. Sci.* **2007**, *62*, 4620.
[51] F. R. Phelan, B. J. Bauer, *Chem. Eng. Sci.* **2009**, *64*, 1747.
[52] M. Schimpf, K. Caldwell, J. C. Giddings, *Field-Flow Fraction Handbook*, Wiley-Interscience Publication, New York **2000**.
[53] M. L. Becker, J. A. Fagan, N. D. Gallant, B. J. Bauer, V. Bajpai, E. K. Hobbie, S. H. Lacerda, K. B. Migler, J. P. Jakupciak, *Adv. Mater.* **2007**, *19*, 939.
[54] J. A. Fagan, V. Bajpai, B. J. Bauer, E. K. Hobbie, *Appl. Phys. Lett.* **2007**, *91*, 213105.
[55] D. Simien, J. A. Fagan, W. Luo, J. F. Douglas, K. Migler, J. Obrzut, *ACS Nano* **2008**, *2*, 1879.
[56] J. L. Blackburn, T. M. Barnes, M. C. Beard, Y. H. Kim, R. C. Tenent, J. McDonald, B. To, T. J. Coutts, M. J. Heben, *ACS Nano* **2008**, *2*, 1266.